Organic & Biomolecular Chemistry

Cite this: *Org. Biomol. Chem.*, 2012, **10**, 6350

www.rsc.org/obc

PAPER

Modification in the side chain of solomonsterol A: discovery of cholestan disulfate as a potent pregnane-X-receptor agonist†

Valentina Sepe,[a] Raffaella Ummarino,[a] Maria Valeria D'Auria,[a] Gianluigi Lauro,[b] Giuseppe Bifulco,[b] Claudio D'Amore,[c] Barbara Renga,[c] Stefano Fiorucci‡[c] and Angela Zampella‡*[a]

Received 26th April 2012, Accepted 1st June 2012
DOI: 10.1039/c2ob25800e

Seven synthetic analogues of the PXR (pregnane-X-receptor) potent natural agonist solomonsterol A were prepared by total synthesis. Their activity toward PXR was assessed by transactivation and RT-PCR assays. The study discloses cholestan disulfate (**8**) as a new, simplified agonist of PXR. By *in vitro* studies on hepatic cells we have demonstrated that this compound is a potent PXR agonist and functional characterization in human macrophages and hepatic stellate cells provided evidence that cholestan disulfate (**8**) has the ability to modulate the immune response triggered by bacterial endotoxin as well as to counter-activate hepatic stellate cell activation induced by thrombin. Because inhibition of immune-driven circuits might have relevance in the treatment of inflammation and liver fibrosis, the present data support the development of cholestan disulfate (**8**) in preclinical models of inflammatory diseases.

Introduction

PXR (pregnane-X-receptor) is a master gene regulating the activity of a variety of genes involved in xeno- and endo-biotic metabolism in the liver and gastrointestinal tract,[1–4] thus preventing toxic accumulation of metabolites within cells.

Once activated, PXR heterodimerizes with the retinoid-X-receptor (RXR), and binds to regulatory DNA sequences in the promoter of responsive genes modulating their transcription. In addition, PXR is recognized as an important regulatory factor for modulation of important effector functions in the immune system through inhibition of pro-inflammatory transcription factor NF-κB in epithelial and immune cells.[5,6] A role for PXR in the pathogenesis of inflammatory bowel disease (IBD) is increasingly supported by genetic and pharmacological evidences. Thus, gene expression analysis of colon tissues from patients with ulcerative colitis and Crohn's disease has revealed a significant reduction in the expression/function of PXR and its target genes compared with normal intestinal samples.[7] Moreover rifaximin, a human PXR activator, is in clinical trials for treatment of IBD and has demonstrated efficacy in Crohn's disease and active ulcerative colitis.[8,9] It is speculated that by activating PXR, rifaximin could contribute to the maintenance of the intestinal barrier integrity by regulating the metabolism of xenobiotics and increasing the expression and activity of PXR and PXR-regulated genes.[10]

Therefore PXR represents an important pharmacological target, and the discovery of potent and selective PXR agonists holds potential in the identification of new drugs for the treatment of human disorders characterized by dysregulation of innate immunity.

Results and discussion

Recently our research group reported the biochemical decodification of several steroids of marine origin as ligands of two nuclear receptors, FXR and PXR.[11–17] Among these, two sulfated steroids, solomonsterols A (**1**) and B isolated from the sponge *Theonella swinhoei*,[18] were proved to be potent inducers of PXR transactivation in human hepatocyte cell line (HepG2 cells) stimulating the expression of CYP3A4 and MDR1 (cytochrome P450 3A4 and multidrug resistance 1), two well characterized PXR responsive genes in the same cell line.[19] In addition, through a deep pharmacological investigation on transgenic mice expressing the human PXR, we have demonstrated that solomonsterol A (**1**) effectively protects against the development of clinical signs and symptoms of colitis, reduces the generation of TNFα and enhances the expression of TGFβ and IL-10, two potent counter-regulatory cytokines in IBD, *via* inhibition of NF-κB activation in a PXR dependent mechanism.[20]

[a]*Dipartimento di Chimica delle Sostanze Naturali, Università di Napoli "Federico II", via D. Montesano 49, 80131 Napoli, Italy. E-mail: angela.zampella@unina.it; Fax: (+0039) 081-678552; Tel: (+0039) 081-678525*
[b]*Dipartimento di Scienze Farmaceutiche e Biomediche, Università di Salerno, via Ponte don Melillo, 84084 Fisciano (SA), Italy*
[c]*Dipartimento di Medicina Clinica e Sperimentale, Università di Perugia, Nuova Facoltà di Medicina e Chirurgia, Via Gerardo Dottori 1, S, Andrea delle Fratte 06132 Perugia, Italy*

†Electronic supplementary information (ESI) available: 1D NMR spectra for compounds **2–10** and HPLC traces. See DOI: 10.1039/c2ob25800e

‡Contributed equally to this work.

All these data pointed towards the identification of solomonsterol A (**1**) as a new lead in the treatment of IBD. One of the possible limitations for its use in clinical settings is that, when administered *per os*, solomonsterol A (**1**) could undergo absorption from the GIT before reaching the colon, causing severe systemic side effects resulting from the activation of PXR in the liver.

solomonsterol A (**1**) to 5-ASA (5-aminosalicylic acid), one of the oldest anti-inflammatory agents in use for the treatment of IBD, could produce a dual-drug with enhanced potency. Upon enzymatic hydrolysis in the colon, this kind of molecule could release solomonsterol A and 5-ASA, potent agonists of PXR and PPARγ,[21] respectively, two nuclear receptors playing a key role in colon inflammation diseases.

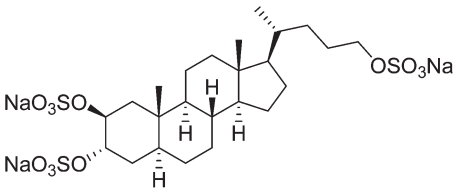

Solomonsterol A (**1**)

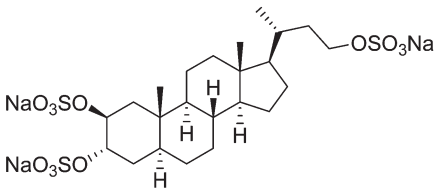

Solomonsterol B

One of the best approaches used for colon specific drug delivery is based on the formation of a prodrug through chemical modification of the drug structure, usually by conjugation with a suitable carrier, such as amino acids, sugars, glucuronic acid, dextrans or polysaccharides.

Since a luxuriant microflora is present in the colon, the prodrug undergoes enzymatic biotransformation in the colon thus releasing the active drug molecule.

Another challenging task is the design of a dual-drug able to release in the colon two molecules acting in a synergic manner. For example the possible eventual chemical linkage of

When synthesizing prodrugs, the first step is the introduction of a functional group on the drug molecule suitable for conjugation with a selected carrier (*e.g.*, an hydroxyl group that could enter into a glycoside linkage with various sugars, or alternatively a carboxyl group to form ester and/or amide conjugates with cyclodextrins, amino acids *etc.*).

Inspection of the chemical structure of solomonsterol A (**1**) revealed that the presence of three sulfate groups hampered any further derivatization and/or conjugation. In order to introduce a functional group suitable for further derivatization, we decided to prepare several solomonsterol A (**1**) derivatives with a

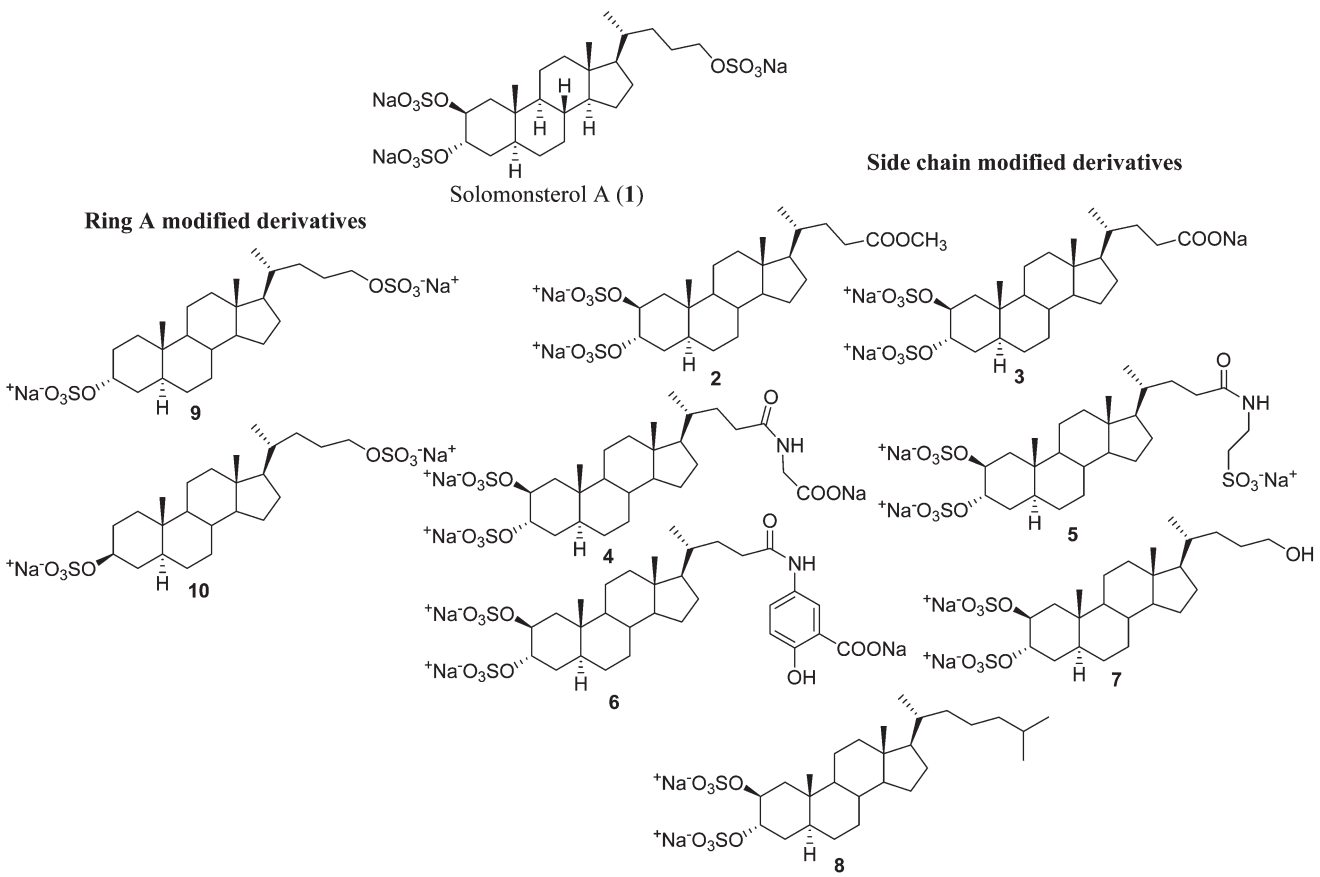

Fig. 1 Solomonsterol A derivatives.

modified side chain but preserving the steroidal tetracyclic nucleus (compounds **2–8** in Fig. 1). Moreover we had also the opportunity to speculate on the pharmacophoric role played by ring A by preparing derivatives **9–10** with a sulfate group at C-3 in α and β orientation, respectively.

The small library of derivatives obtained (Fig. 1) was subjected to pharmacological evaluation and docking analysis. This study led to the discovery of a synthetic solomonsterol A analogue, 2β,3α-cholestan disulfate (**8**), as a simplified new potent PXR agonist.

Chemistry and biological evaluation

Our synthetic route started from the advanced intermediate **11**[20] that was sulfated with 10 equivalents of triethylammonium–sulfur trioxide complex and transformed into the sodium sulfate salt **2** through Amberlite treatment. The crude product was subsequently hydrolyzed with methanolic NaOH (5%) to remove the protecting group at the C-24, affording the desired carboxylic acid functional group. The reaction mixture was adjusted to pH 5 with HCl 1N, and loaded onto a C18 cartridge for reversed-phase solid extraction (Scheme 1).

Elution with 30% aqueous methanol gave the carboxylic acid **3** as a 2,3,24-trisodium salt in satisfactory yield (85% over two steps).

With the carboxylate (**3**) in our hands, we decided to carry on with the reaction of amidation with glycine ethyl ester, taurine and 5-ASA. Using a versatile coupling agent, DMT-MM [4-(4,6-dimethoxy-1,3,5-triazin-2-yl)-4-methylmorpholinium chloride],[22] the amidation reaction proceeded nearly quantitatively, requiring the activation of the carboxylate sodium salt by DMT-MM and triethylamine in DMF at room temperature, and subsequent condensation of the resulting acyloxytriazine with glycine ethyl ester hydrochloride, taurine or 5-ASA afforded the amide derivatives **12**, **5** and **6** respectively, as ammonium sulfate salts. Alkaline hydrolysis of ethylester **12** with NaOH 5% in MeOH–H_2O 1 : 1 afforded the sodium carboxylate **4**.

Amide derivatives with taurine and 5-ASA were transformed *via* ion exchange (Amberlite CG-120, sodium form, MeOH) into the desired target trisodium salts **5** and **6** in good yields.

To investigate whether compounds **3–6** act on PXR and eventually PXR regulated genes, we carried out a luciferase reporter assay on human hepatocyte cell line (HepG2 cells) transiently transfected with pSG5-PXR, pSG5-RXR, pCMV-βgalactosidase, and p(CYP3A4)-TK-Luc vectors (Fig. 2). Cells were then stimulated with rifaximin, a well known PXR agonist, and with compounds **3–6** at a concentration of 10 μM each. As shown in Fig. 2A, despite the close structural resemblance with solomonsterol A (**1**), only carboxylate (**3**) showed a slight activity in transactivating PXR. Besides at first sight this behaviour could be ascribable to scarce bioavailability, the scarce activity also obtained for the methyl ester **2** (Fig. 2A) and the complete loss of activity for C-24 alcohol **7** (Fig. 2A), obtained through $LiBH_4$ reduction of **2** (75% yield), pointed towards unfavourable

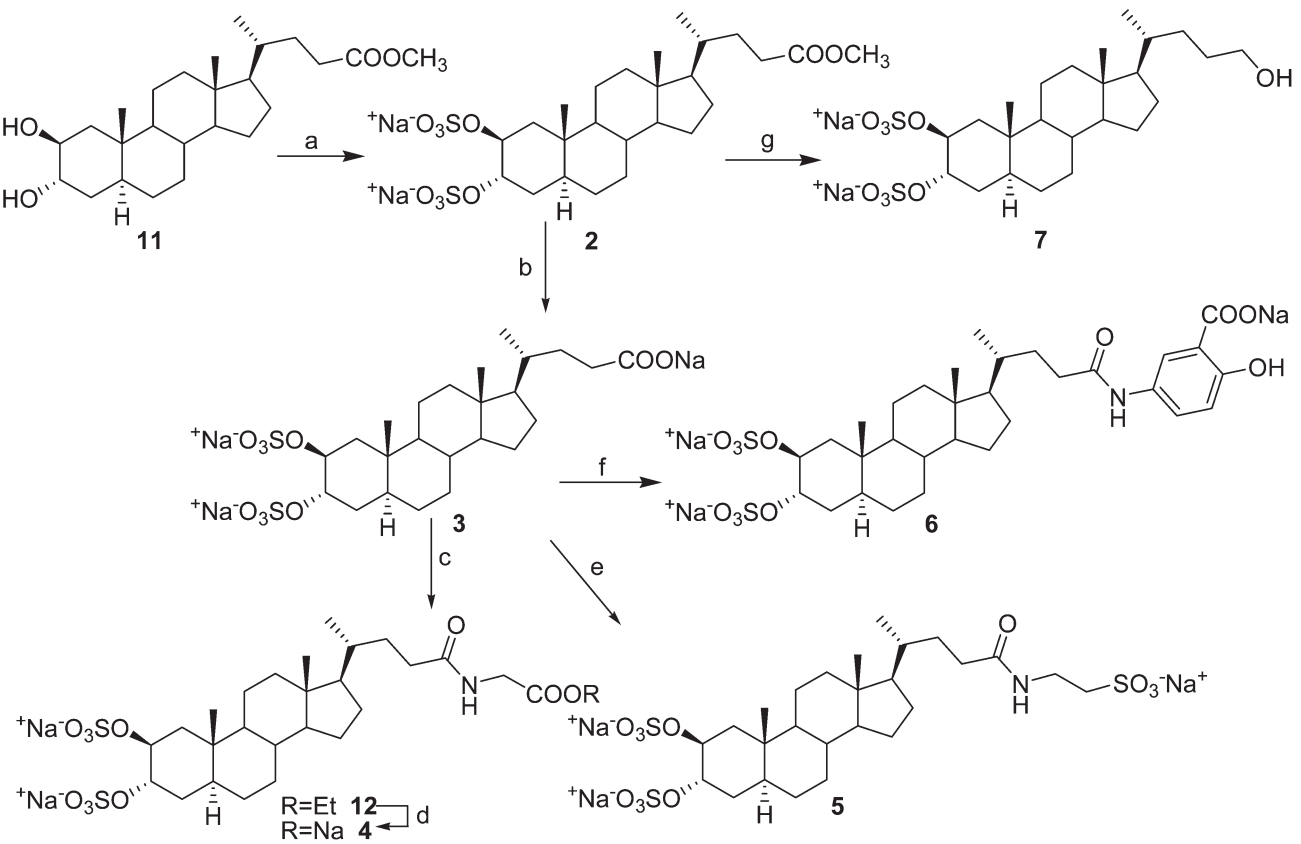

Scheme 1 (a) $Et_3N{\cdot}SO_3$, DMF, 95 °C; (b) NaOH 5% in MeOH–H_2O 5 : 1 v/v, 85% over two steps; (c) DMT-MM, Et_3N, GlyOEt, dry DMF; (d) NaOH 5% in MeOH–H_2O 5 : 1 v/v, 58% over two steps; (e) DMT-MM, Et_3N, taurine, dry DMF. Then Amberlite CG-120, MeOH, 67%. (f) DMT-MM, Et_3N, 5-ASA, dry DMF. Then Amberlite CG-120, MeOH, 72%; (g) $LiBH_4$, MeOH, THF, 0 °C, 75%.

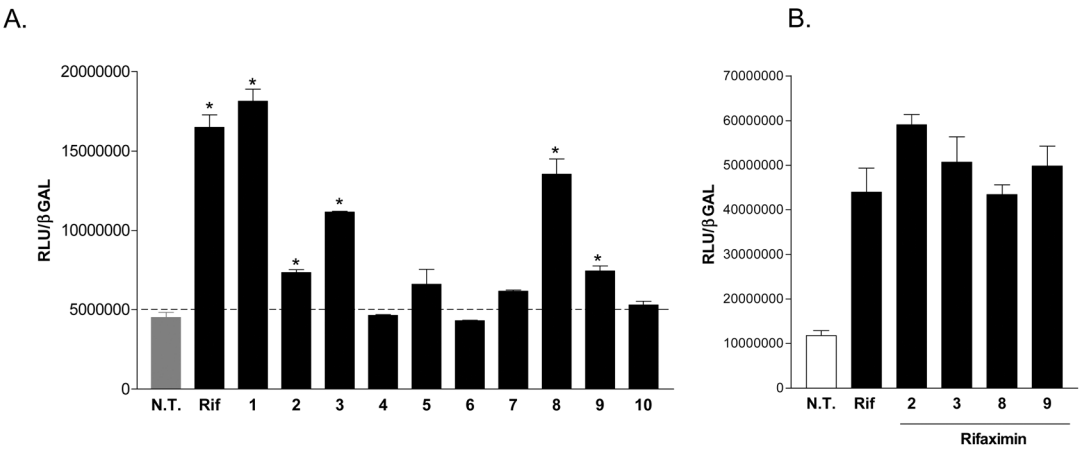

Fig. 2 Luciferase reporter assay. HepG2 cells were transiently transfected with pSG5-PXR, pSG5-RXR, pCMV-βgalactosidase and p(CYP3A4)-TK-Luc vectors and then stimulated with (**A**) 10 μM rifaximin or compounds **1–10** for 18 h, or (**B**) 10 μM rifaximin alone or in combination with 50 μM of compounds **2**, **3**, **8** and **9**. N.T., not treated. Rif, rifaximin. *$P < 0.05$ *versus* cells left untreated. Data are mean ± SE of three determinations.

pharmacodynamic features. Indeed, although compounds **3–6** possess a negative charge on their side chains, most likely they are less able to form polar interactions with Lys210[20] or alternatively with other polar amino acids of PXR LBD.

As previously reported, PXR presents a large ligand binding cavity[23,24] allowing the accommodation of different kind of molecules, and the possible binding modes are characterized by an adequate balance between hydrogen bond and Van der Waals interactions established between a small molecule and the receptor.

Therefore the lack of a polar interaction should be overcome by increasing the contribution of the hydrophobic interactions on the side chain and so the derivative **8**, 2β,3α-cholestan disulfate was prepared according to the synthetic procedure reported in Scheme 2.[25] Δ^5 cholesterol reduction (H_2, Pd/C, THF–MeOH 1 : 1) followed by tosylation and LiBr elimination afforded Δ^2-cholestane derivative **13** (78% yield in three steps). The introduction of the 2β,3α-dihydroxy functionality was achieved by epoxidation with *m*-CPBA followed by acid catalyzed ring opening of epoxide **14**.[26] β-Elimination and epoxidation proceeded with excellent regioselectivity and stereoselectivity, providing exclusively the desired 2β,3α-diol **15** in excellent yields (78% over two steps).

Sulfination of diol **15** followed by Amberlite CG-120 treatment and RP-18 chromatography afforded the disodium salt **8** in good yields. As shown in Fig. 2A, compound **8** with its hydrophobic side chain is able to transactivate PXR with a potency comparable with the parent solomonsterol A (**1**).

Having set a flexible synthetic strategy, we decided to speculate on the pharmacophoric role played by the sulfate groups on ring A in the PXR agonistic activity of solomonsterol A (**1**).

Tosylation of methyl 3β-hydroxy-5α-cholan-24-oate (**16**)[20] followed by inversion of configuration at C-3 with potassium

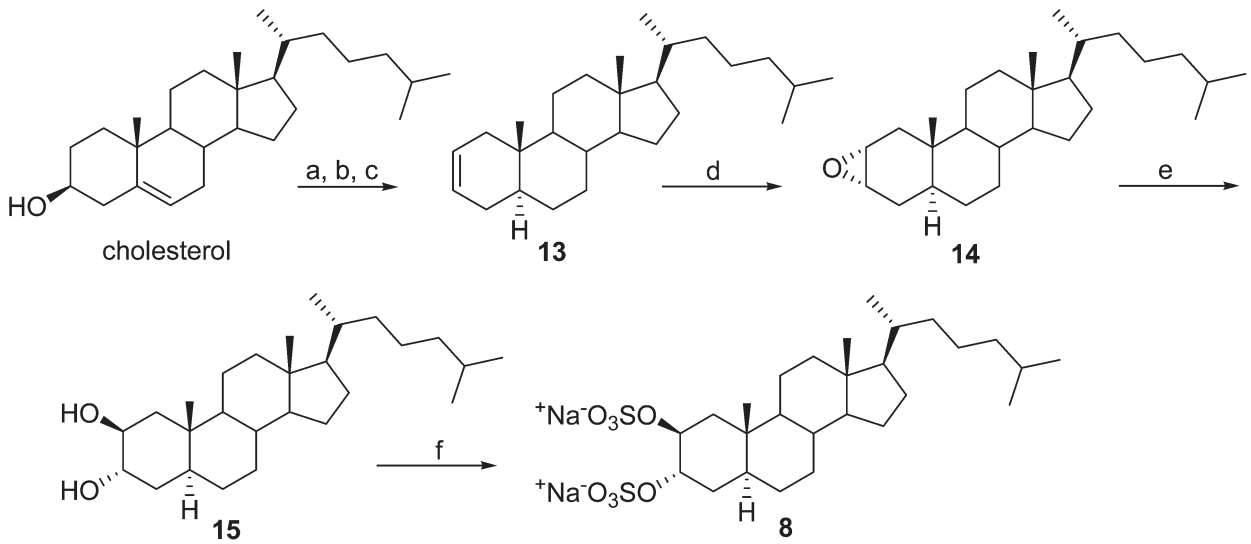

Scheme 2 (a) H_2, Pd/C, THF–MeOH 1 : 1, room temperature, 90%; (b) *p*-TsCl, pyridine; (c) LiBr, Li_2CO_3, DMF, reflux, 87% over two steps; (d) *m*-CPBA, $CHCl_3$ room temperature; (e) H_2SO_4 1 N, THF, room temperature, 78% over two steps; (f) $Et_3N{\cdot}SO_3$, DMF, 95 °C. Then Amberlite CG-120, MeOH, 90%.

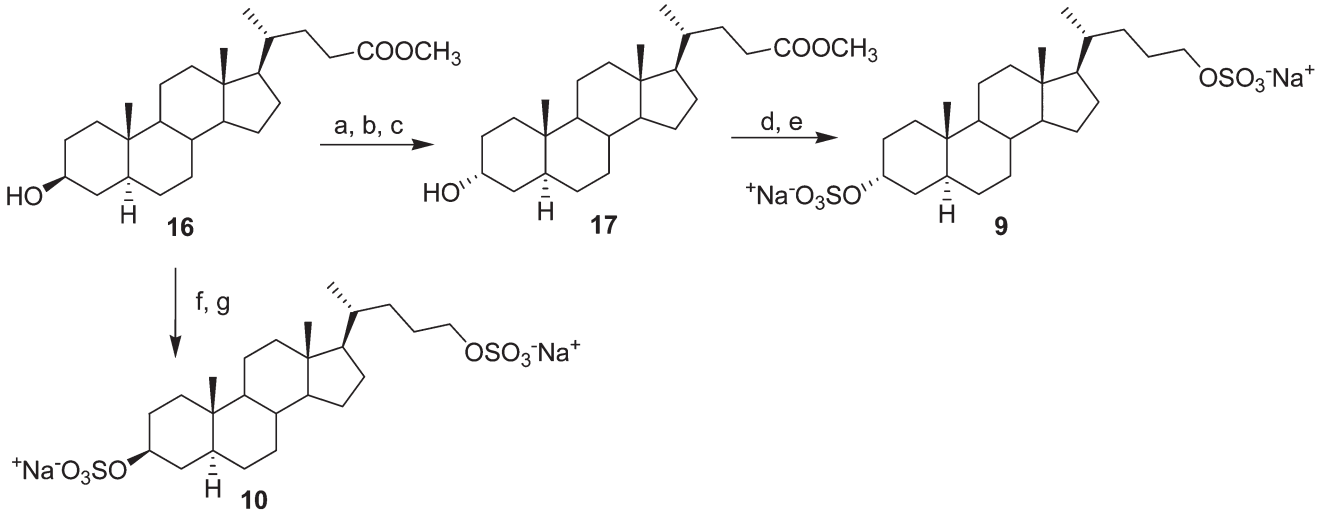

Scheme 3 (a) *p*-TsCl, pyridine; (b) CH_3COOK, DMF–H_2O 9 : 1, reflux; (c) *p*-TsOH, $CHCl_3$–MeOH 5 : 3, 75% over three steps; (d) $LiBH_4$, MeOH, THF, 0 °C, 85%; (e) $Et_3N{\cdot}SO_3$, DMF, 95 °C; then Amberlite CG-120, MeOH, 63%; (f) $LiBH_4$, MeOH, THF, 0 °C, 72%; (g) $Et_3N{\cdot}SO_3$, DMF, 95 °C; then Amberlite CG-120, MeOH, 78%.

acetate in DMF–H_2O and de-acetylation in acidic conditions (Scheme 3) afforded the 3α-hydroxy derivative **17** (75% over three steps). Reduction at C-24, sulfination/Amberlite ion exchange gave the disodium salt **9**.

Methyl 3β-hydroxy-5α-cholan-24-oate (**16**) was also used as the starting material for the easy transformation into derivative **10** through $LiBH_4$ reduction of the C-24 methyl ester and successive sulfination of the alcoholic functions at C-3 and C-24.

As indicated in Fig. 2A, although compound **9** induces a slight PXR transactivation, the lack of sulfate group at C-2 as well as the inversion of configuration at C-3 are responsible for a general loss in the agonistic activity towards PXR.

To investigate whether these compounds could act as potential antagonists of PXR we have carried out a transactivation experiment in HepG2 cells stimulated with rifaximin (10 μM) and compounds **2**, **3**, **8** and **9** at a concentration of 50 μM each. As shown in Fig. 2B, all compounds failed to reverse the induction of luciferase caused by rifaximin, indicating that none of these solomonsterol A (**1**) derivatives is a PXR antagonist.

To further examine the activity of compound **8** as a PXR activator and further clarify the behavior of compounds **2**, **3** and **9**, we have tested the effects of all members of our series on the expression of CYP3A4, a canonical PXR target gene (Fig. 3). Despite compounds **2**, **3** and **9** causing a slight transactivation of PXR, they failed to modulate the expression of CYP3A4 at the concentration of 10 μM. In contrast, confirming data shown in Fig. 2, compound **8** effectively increased the expression of CYP3A4 (Fig. 3) in HepG2 cells, with a magnitude similar to that of rifaximin and solomonsterol A (**1**). While these data do not exclude that compound **3** could also stimulate CYP3A4 expression in this system, the need for higher concentrations to display a full PXR agonistic activity precluded its further development.

To further investigate whether compound **8** displays a full PXR agonistic activity, we then evaluated the effect of **8** in regulating immune response using THP1 cells, a human macrophage/monocytic cell line, challenged with lipopolysaccharide (LPS), a

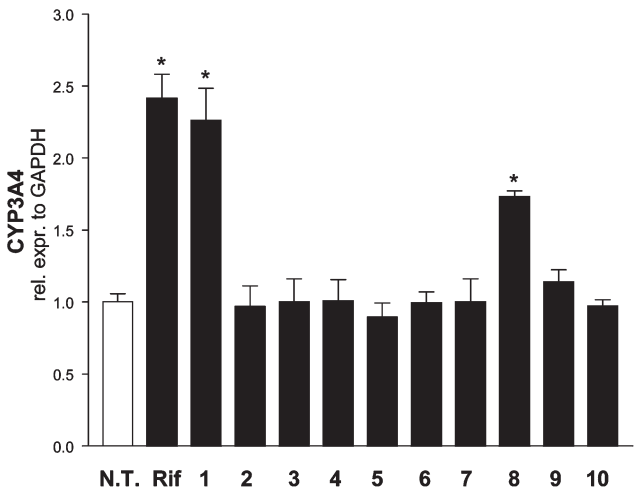

Fig. 3 Real-time PCR of CYP3A4 carried out on cDNA isolated from HepG2 not stimulated or primed with 10 μM rifaximin, and compounds **1–10**. N.T., not treated. Rif, rifaximin. *$P < 0.05$ *versus* N.T. cells.

potent agonist of Toll like receptor (TLR)-4. Previous studies[27] have shown that activation of PXR in this setting attenuates immune response triggered by LPS. Data shown in Fig. 4, demonstrate that compound **8** effectively attenuates induction of IL-1β, TNFα and MCP-1 induced by LPS.

Because the above mentioned data indicate that compound **8** effectively modulates immune response in human monocytes, additional experiments were carried out to investigate the effect of this compound in another model of inflammation-driven activation, using hepatic stellate cells (HSCs). HSCs are a liver-resident cell population that proliferate in response to liver injury. In response to immune activation, HSCs undergo a complex phenotype rearrangement characterized by resetting expression of nuclear receptors, including PXR, and acquisition of an activated, myofibroblast-like phenotype whose main characteristic is the ability to express α-smooth muscle actin (αSMA). HSCs are

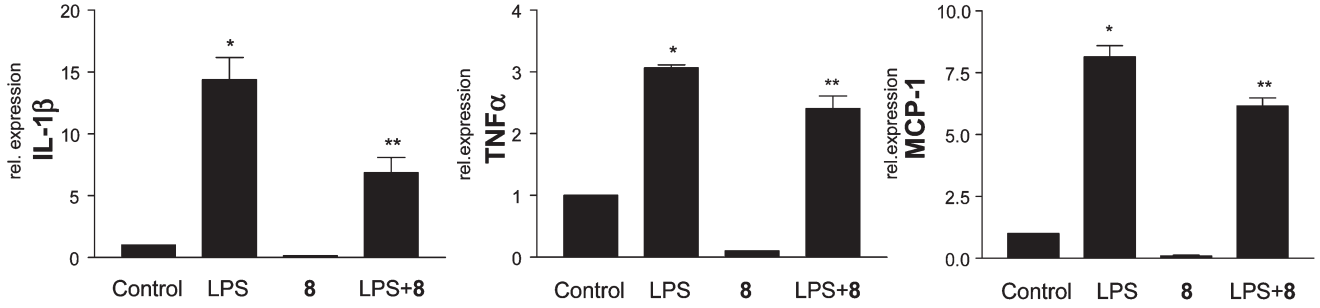

Fig. 4 Effect of compound **8** on cytokine release induced by LPS in THP1 cells. 3×10^6 THP were starved for 24 h and then pre-treated with 10 μM of compound **8** for 3 h and then stimulated for 18 h with LPS 1 μg mL^{-1}. Cytokine expression was assessed by RT-PCR. Data shown are mean ± SE of 9 assays from three different sets of experiments. *$P < 0.05$ *versus* control cells; **$P < 0.05$ *versus* LPS alone.

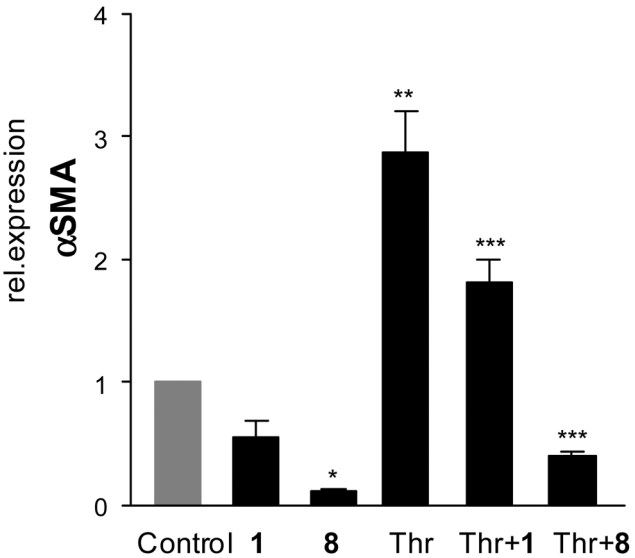

Fig. 5 HSC-T6 cells were starved for 72 h and then stimulated with thrombin, 10 U mL^{-1}, in the presence of solomonsterol A (**1**) or compound **8**, 10 μM each. αSMA expression was assessed by RT-PCR. Data shown are mean ± of three experiments. *$P < 0.05$ *versus* control cells; **$P < 0.05$ thrombin *versus* control cells; ***$P < 0.05$ *versus* thrombin alone.

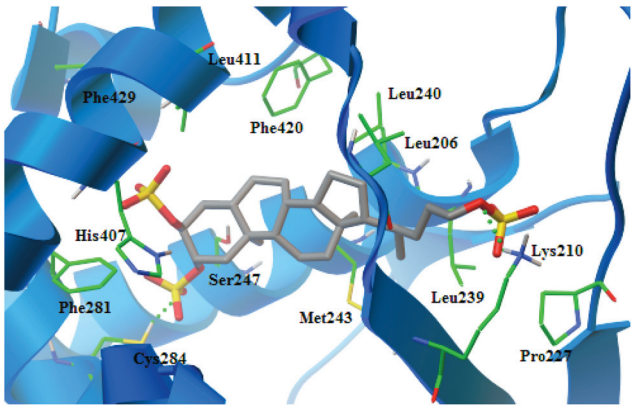

Fig. 6 Solomonsterol A (**1**) (coloured by atom types: C grey, O red, S yellow) in docking with PXR-LBD (residues are coloured by atom type: C green, H light grey, O red, N blue). Hydrogen bonds are displayed with green spheres.

recognized as the main source of extracellular matrix production in the fibrotic liver. Previous studies have shown that, along with other nuclear receptors, PXR ligands reverse this phenotype and reduce α-SMA expression.[28–30] For this purpose HSCs were exposed to thrombin, a proteinase activated receptor (PAR)-1 agonist alone or in combination with compound **8**. Previous studies have shown that thrombin drives HSCs trans-differentiation and its inhibition reverses HSCs from an activated to a quiescent phenotype.[31] Results shown in Fig. 5 demonstrate that, similarly to solomonsterol A (**1**), not only does compound **8** effectively reduce basal expression of αSMA, but it also attenuates HSCs trans-differentiation (*i.e.* induction of αSMA expression) triggered by thrombin.

Docking studies

In order to clarify the different activities of the compounds described here at a molecular level, we performed docking calculations, using the Autodock 4.2 software,[32] thus examining the positioning of all the compounds in the binding site of PXR,[33] and in particular we analyzed the crucial interactions with the Ser247, His407 and finally with the Lys210. These residues, in particular the Ser247, are involved in hydrogen bonds with various PXR ligands.[24,33,34] The three sulfate groups of the agonist solomonsterol A (**1**) act as key points of interaction with these amino acids, and contribute to accommodating the steroid nucleus in a mostly hydrophobic part of the binding site of PXR. Solomonsterol A (**1**) establishes hydrogen bonds (Fig. 6) with the Cys284 (2-*O*-sulfate) and with the Lys210 (24-*O*-sulfate) and electrostatic interactions with the Ser247 (2-*O*-sulfate) and His407 (3-*O*-sulfate).[20]

Compound **8**, featuring the C8 aliphatic side chain of cholesterol, is well superimposed with the binding pose of **1**, and is able to interact with the Ser247, Cys284 and the His407 through its two sulfate groups in the ring A (Fig. 7). Moreover, **8** establishes hydrophobic interactions with almost all the residues observed for solomonsterol A (**1**) (Leu209, Val211, Pro228, Leu239, Met243, Phe281, Phe288, Leu411). The presence of hydrophobic chain allows the gaining of two more Van der Waals interactions (with the Leu209 and Val211) that may counter the loss of electrostatic interaction observed for the sulfate group at C24 of parent solomonsterol A (**1**). Nevertheless,

the weaker nature of these Van der Waals interactions could explain the decrease of the activity of **8** on PXR (difference of predicted binding energies **1**–**8** = 1.05 kcal mol^{-1}).

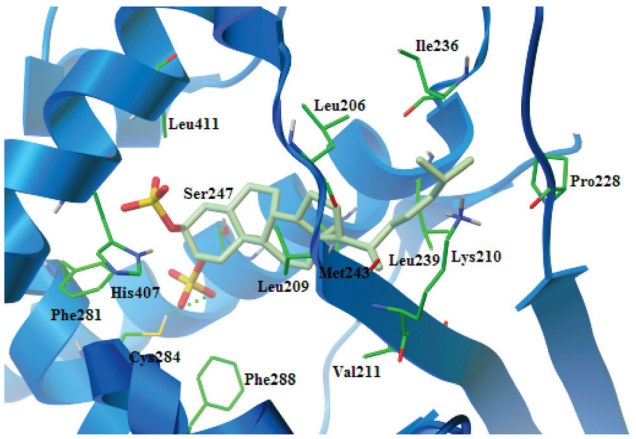

Fig. 7 Compound **8** (coloured by atom types: C light green, O red, S yellow) in docking with PXR-LBD (residues are coloured by atom type: C green, H light grey, O red, N blue). Hydrogen bonds are displayed with green spheres.

On the other hand, the absence of the sulfate group at C-2 in the steroid nucleus causes the observed decrease of activity, due to an inability to interact simultaneously with the three key points of contact previously described. For example, compounds **9** and **10** are able to interact with the Lys210 but they fail to respect the key interactions involving the internal part of the binding site (Fig. 8). Concerning compound **3**, its tetracyclic nucleus is well superimposed with **1**, but its shorter side chain causes a poor interaction with the nitrogen of Lys210. The two oxygens of its terminal carboxylic part are not well overlapped with the oxygens of the 24-*O*-sulfate of **1**, and the different arrangement of the side chain causes also a loss of two Van der Waals interactions with the Leu239 and Pro227 (Fig. 8). In other cases a displacement of the compounds to the solvent part is observable. For example, the rings A of compounds **2** and **7** are in the place occupied by the ring B of **1** and, as a consequence, the 2-*O*-sulfate and/or 3-*O*-sulfate are in a less deep position (Fig. 8). Compounds **4**, **5** and **6** present a longer and more functionalized side chain (Fig. 8) compared with the previous derivatives, but also in these cases the steroid nucleus is placed toward the external part of the binding site of PXR (**4**, **6**). Moreover, compound **5** is unable to bind in the above described fashion and accommodates its steroid nucleus in a reverse orientation

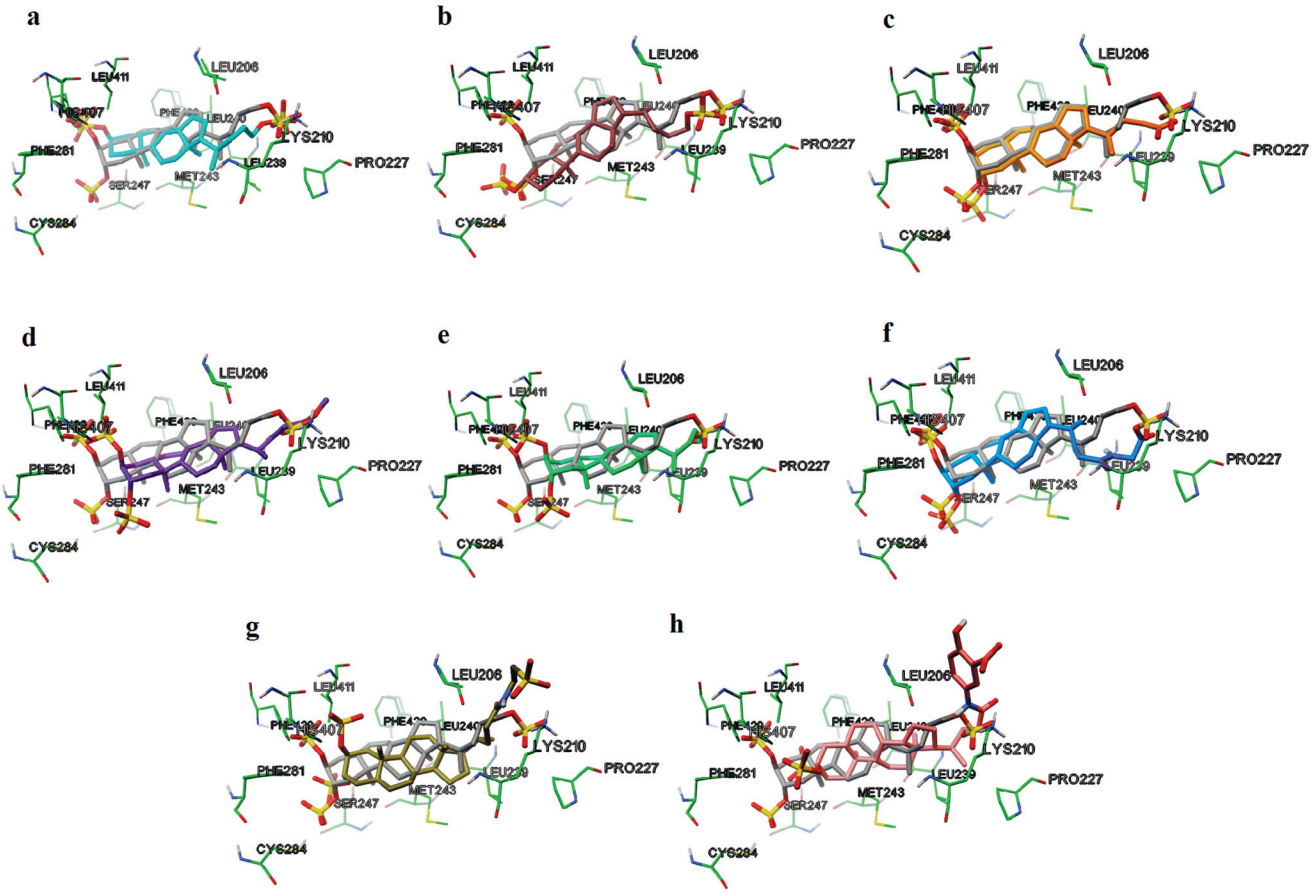

Fig. 8 Superimposition between **1** (coloured by atom types: C grey, O red, S yellow) and: (a) **9** (coloured by atom types: C sky-blue, O red, S yellow); (b) **10** (coloured by atom types: C brown, O red, S yellow); (c) **3** (coloured by atom types: C orange, O red, S yellow); (d) **2** (coloured by atom types: C purple, O red, S yellow); (e) **7** (coloured by atom types: C turquoise green, O red, S yellow); (f) **4** (coloured by atom types: C dodger blue, O red, S yellow); (g) **5** (coloured by atom types: C dark green, O red, S yellow); (h) **6** (coloured by atom types: C pink, O red, S yellow) in PXR-LBD (residues are coloured by atom type: C green, H light grey, O red, N blue).

(a flipping of ~180° along the major axis of the steroid nucleus) (Fig. 8). The overall result is an inverted disposition of all the chemical groups (sulfates/methyl groups, and side chain) in the binding pocket of PXR and therefore a different pattern of interactions.

Conclusion

In this study we report the synthesis of several derivatives of solomonsterol A (**1**), a potent agonist of PXR of marine origin and a new lead in the treatment of IBD. Biochemical characterization of these analogues, modified in the side chain and in the ring A, allowed us to delineate a first SAR and, notably, to identify a simplified derivative, cholestan disulfate (**8**) as a new PXR agonist. The ability of this compound to act as a PXR agonist was first demonstrated in a transactivation assay using HepG2 cells transiently transfected with a PXR vector. The results of these experiments demonstrate that compound **8**, and less effectively compounds **2**, **3** and **9**, efficiently transactivates human PXR with a relative potency that was very similar to that of rifaximin, a well characterized PXR agonist. Moreover, in agreement with transactivation experiments, the PCR data demonstrate that compound **8** increases the expression of CYP3A4, a well characterized PXR responsive gene, in liver cells. The functionality of the interaction of compound **8** with PXR was further investigated in two different cell models. Using THP1 cells, a monocytic cell line, we have provided evidence that compound **8** attenuates cytokine generation induced by LPS. Because previous studies have provided robust evidence that PXR activation by rifaximin and solomonsterol A[20] exerts anti-inflammatory activity in rodent models of colitis by attenuating inflammation driven-immune dysfunction and cytokine accumulation in inflamed tissues, the present results extend on the role of PXR ligands in regulating immune function, and pave the way for the use of compound **8** in preclinical models of inflammation. Despite the fact that we have not investigated the mechanism mediating inhibition of cytokines by compound **8**, we and others have provided evidence that PXR agonists inhibit NF-κB activation.[20,35]

Extending on the role of PXR as an endogenous braking signal for inflammation, we have then examined whether compound **8** would have been effective in reducing collagen production by HSCs, a myofibroblast-like cell line. HSCs acquire an activated phenotype in response to liver injury and release collagen and express αSMA in response to toxic and immunological stimuli in a variety of liver disorders. Previous studies have provided evidence that nuclear receptors, including FXR, SHP and PPARγ, modulate a collagen release by HSCs and might function as important therapeutic targets for treating liver fibrosis.[36] PXR ligation attenuates liver fibrosis and HSCs activation.[37] Here we have shown that solomonsterol A (**1**) and compound **8** reduce αSMA accumulation triggered by thrombin. There is substantial evidence to support the notion that PXR activators are anti-fibrogenic in human liver myofibroblasts *in vitro*[38] and in *in vivo* animal models of liver fibrosis.[28–30] The role of the PXR in regulating HSCs activation has been unequivocally established using mice with a disrupted PXR gene.[28] The mechanism throughout which PXR regulates production of extracellular matrix proteins is likely associated with a function for the PXR that is not related with its recognized function as a regulator of genes associated with endobiotic and xenobiotic clearance, and might be linked to inhibition of intracellular signaling including NF-κB, or involved in the regulation of trans-differentiation of these fat-storing cells as demonstrated for other nuclear receptors including PPARγ and farnesoid-X-receptor, FXR.[39]

In summary, in the present study we report on the generation of a series of derivatives of solomonsterol A (**1**), a marine steroid that acts as a PXR agonist. By transactivation assay and pharmacological characterization we have shown that compound **8** is a robust PXR agonist that modulates immune response in human macrophages. Because of its simplified structure and efficacy in attenuating immune activation in macrophages and HSCs, compound **8** is a suitable candidate for further development in preclinical models of inflammatory diseases. Further studies aimed at the evaluation of efficacy of **8** in animal models, together with the determination of its chemical–physical proprieties, are currently in progress.

Experimental

Specific rotations were measured on a Perkin-Elmer 243 B polarimeter. High-resolution ESI-MS spectra were performed with a Micromass QTOF Micromass spectrometer. ESI-MS experiments were performed on an Applied Biosystem API 2000 triple-quadrupole mass spectrometer. NMR spectra on all synthetic intermediates were obtained on Varian Inova 400 and Varian Inova 500 NMR spectrometers (^{1}H at 400 and 500 MHz, ^{13}C at 100 and 125 MHz, respectively) and recorded in $CDCl_3$ (δ_H = 7.26 and δ_C = 77.0 ppm) and CD_3OD (δ_H = 3.30 and δ_C = 49.0 ppm).

HPLC was performed using a Waters Model 510 pump equipped with Waters Rheodine injector and a differential refractometer, model 401.

Reaction progress was monitored *via* thin-layer chromatography (TLC) on Alugram silica gel G/UV254 plates. Silica gel MN Kieselgel 60 (70–230 mesh) from Macherey-Nagel Company was used for column chromatography. All chemicals were obtained from Sigma-Aldrich Inc. Solvents and reagents were used as supplied from commercial sources with the following exceptions. Tetrahydrofuran, chloroform and triethylamine were distilled from calcium hydride immediately prior to use. All reactions were carried out under argon atmosphere using flame-dried glassware.

The purities of compounds were determined to be greater than 95% by HPLC.

Diol **11** was prepared according to the synthetic procedure previously described.[20] An analytical sample was obtained by HPLC on a Nucleodur 100-5 C18 (5 μm; 4.6 mm i.d. × 250 mm, MeOH–H_2O 87 : 13, flow rate 1.5 mL min^{-1}, t_R = 2.6 min).

Synthetic procedures

Methyl 2β,3α-disulfate-5α-cholan-24-oate (2). Triethylamine–sulfur trioxide complex (1.34 g, 7.4 mmol) was added to diol **11**

(300 mg, 0.74 mmol) in DMF dry (10 mL) under an argon atmosphere, and the mixture was stirred at 95 °C for 48 h. The reaction mixture was quenched with water (1.6 mL) and the solution was poured over a C18 silica gel column to remove excess $Et_3N{\cdot}SO_3$. The product was eluted by MeOH and followed by evaporation of the solvent to yield a yellow solid [bis-(triethylammonium sulfate) salt]. To the solid dissolved in methanol (30 mL) was added Amberlite CG 120 sodium form (30 g) and the mixture was stirred for 5 h at room temperature. The resin was removed by filtration, and the filtrate was concentrated to obtain compound **2** as a white solid (270 mg, 60%). An analytical sample was obtained by HPLC on a Nucleodur 100-5 C18 (5 µm; 4.6 mm i.d. × 250 mm, MeOH–H_2O 34 : 66, flow rate 1.5 mL min^{-1}, t_R = 3.6 min). $[\alpha]_{24}^{D}$ = +9.6 (*c* 0.08, CH_3OH); selected ^1H NMR (400 MHz CD_3OD): δ 4.69 (1H, br s), 4.66 (1H, br s), 3.61 (3H, s), 2.31 (1H, m), 2.17 (1H, m), 0.96 (3H, s), 0.90 (3H, d, *J* = 6.5 Hz), 0.66 (3H, s); ^{13}C NMR (100 MHz CD_3OD): 176.5, 76.5, 76.1, 57.8, 57.4, 56.3, 51.8, 43.8, 41.4, 40.3, 39.1, 36.8, 36.5, 36.4, 33.2, 32.5, 32.4, 30.5, 29.1 (2C), 25.2, 21.9, 18.8, 14.3, 12.5. HR ESIMS *m/z* 587.1975 $[M - Na]^-$, $C_{25}H_{40}NaO_{10}S_2$ requires 587.1961.

Disodium 2β,3α-disulfate-5α-cholan-24-oic acid (3). Compound **2** (160 mg, 0.26 mmol) was dissolved in 5% methanolic NaOH (10 mL) and water (2 mL) and the solution was refluxed for 5 h. The resulting solution was adjusted to pH 5 and concentrated under reduced pressure. Purification by C18 silica gel column eluting with H_2O–MeOH (99 : 1) gave the carboxylate **3** as a white solid (140 mg, 90%). An analytical sample was obtained by HPLC on a Nucleodur 100-5 C18 (5 µm; 4.6 mm i.d. × 250 mm, MeOH–H_2O 30 : 70, flow rate 1.5 mL min^{-1}, t_R = 3.6 min). $[\alpha]_{24}^{D}$ = +2.7 (*c* 0.3, CH_3OH); selected ^1H NMR (400 MHz CD_3OD): δ 4.73 (1H, br s), 4.69 (1H, br s), 2.31 (1H, m), 2.17 (1H, m), 0.99 (3H, s), 0.94 (3H, d, *J* = 6.0 Hz), 0.69 (3H, s); ^{13}C NMR (100 MHz CD_3OD): δ 178.9, 76.4, 76.1, 57.8, 57.4, 56.5, 43.8, 41.4, 40.2, 39.2, 36.8, 36.4, 36.3, 33.2, 32.5 (2C), 30.5, 29.2 (2C), 25.2, 22.0, 18.7, 14.3, 12.6. ESIMS *m/z* 595.1636 $[M - Na]^-$, $C_{24}H_{37}Na_2O_{10}S_2$ requires 595.1624.

2β,3α-disulfate-5α-cholan-24-oyl glycine trisodium salt (4). Carboxylate **3** (50 mg, 0.08 mmol) in DMF dry (2 mL) was treated with DMT-MM (66 mg, 0.24 mmol) and triethylamine (278 µL) and the mixture was stirred at room temperature for 10 min. Glycine ethyl ester (49.5 mg, 0.48 mmol) was then added to the mixture and stirring was continued for 24 h. After adding 5% methanolic NaOH (5 mL) and stirring for 5 h at room temperature, the alkaline solution was adjusted to pH 5, diluted with water and loaded onto a C18 silica gel column, which was washed with water (50 mL). Elution with 10% methanol gave the compound **4** (31 mg, 58% over two steps). An analytical sample was obtained by HPLC on a Nucleodur 100-5 C18 (5 µm; 4.6 mm i.d. × 250 mm, MeOH–H_2O 30 : 70, flow rate 1.5 mL min^{-1}, t_R = 3.4 min). $[\alpha]_{24}^{D}$ = +10.8 (*c* 0.15, CH_3OH); selected ^1H NMR (400 MHz CD_3OD): δ 4.73 (1H, br s), 4.70 (1H, br s), 3.72 (2H, s), 2.28 (1H, m), 2.13 (1H, m), 1.00 (3H, s), 0.97 (3H, d, *J* = 6.0 Hz), 0.69 (3H, s); ^{13}C NMR (100 MHz CD_3OD): δ 176.5, 172.9, 76.5, 76.2, 57.8, 57.4, 56.6, 44.5, 43.8, 41.4, 40.2, 39.1, 36.9, 36.5, 36.4, 36.3, 34.1, 33.2, 33.1, 30.5, 29.2, 25.2, 22.0, 18.8, 14.3, 12.6. HR ESIMS *m/z* 652.1855 $[M - Na]^-$, $C_{26}H_{40}NNa_2O_{11}S_2$ requires 652.1838.

2β,3α-disulfate-5α-cholan-24-oyl taurine trisodium salt (5). Carboxylate **3** (50 mg, 0.08 mmol) in DMF dry (2 mL) was treated with DMT-MM (66 mg, 0.24 mmol) and triethylamine (278 µL) and taurine (60 mg, 0.48 mmol) was then added to the mixture, which was further stirred for 24 h. Then, the reaction mixture was concentrated under *vacuo* and dissolved in water (5 mL). The solution was poured over a C18 silica gel column. The product was eluted with H_2O–MeOH 99 : 1. To the solution of the solid in methanol (2 mL) was added Amberlite CG 120 sodium form (1 g) and the mixture was stirred for 5 h at room temperature. The resin was removed by filtration, and the filtrate was concentrated to obtain compound **5** as a white solid (39 mg, 67%). An analytical sample was obtained by HPLC on a Nucleodur 100-5 C18 (5 µm; 4.6 mm i.d. × 250 mm, MeOH–H_2O 30 : 70, flow rate 1.5 mL min^{-1}, t_R = 3.4 min). $[\alpha]_{24}^{D}$ = +7.1 (*c* 0.22, CH_3OH); selected ^1H NMR (400 MHz CD_3OD): δ 4.73 (1H, br s), 4.70 (1H, br s), 3.57 (2H, t, *J* = 7.0 Hz), 2.95 (2H, t, *J* = 7.0 Hz), 2.23 (1H, m), 2.07 (1H, m), 0.99 (3H, s), 0.95 (3H, d, *J* = 6.4 Hz), 0.68 (3H, s); ^{13}C NMR (100 MHz CD_3OD): δ 176.7, 76.5, 70.5, 57.9, 57.3, 56.5, 51.5, 43.9, 41.4, 40.2 (2C), 39.2, 36.9, 36.6, 36.4, 36.3, 34.2, 33.2, 33.1, 30.5, 29.1, 25.1, 22.0, 18.8, 14.3, 12.6. HR ESIMS *m/z* 702.1685 $[M - Na]^-$, $C_{26}H_{42}NNa_2O_{12}S_3$ requires 702.1665.

Trisodium 2β,3α-disulfate-5α-cholan-24-oyl 5-aminosalycilic acid (6). Carboxylate **3** (50 mg, 0.08 mmol) in DMF dry (2 mL) was treated with DMT-MM (66 mg, 0.24 mmol), triethylamine (278 µL) and 5-aminosalicylic acid (5-ASA) (73 mg, 0.48 mmol) as described for compound **5** to obtain **6** as a white solid (43.3 mg, 72%). An analytical sample was obtained by HPLC on a Nucleodur 100-5 C18 (5 µm; 4.6 mm i.d. × 250 mm, MeOH–H_2O 30 : 70, flow rate 1.5 mL min^{-1}, t_R = 3.4 min). $[\alpha]_{24}^{D}$ = +8.2 (*c* 1.8, CH_3OH); selected ^1H NMR (400 MHz CD_3OD): δ 7.71 (1H, d, *J* = 3.1 Hz), 7.6 (1H, dd, *J* = 3.1 and 8.7 Hz), 6.7 (1H, d, *J* = 8.7 Hz), 4.75 (1H, br s), 4.72 (1H, br s), 2.39 (1H, m), 2.25 (1H, m), 1.02 (3H, d, *J* = 6.0 Hz), 1.01 (3H, s), 0.72 (3H, s); ^{13}C NMR (100 MHz CD_3OD): δ 181.2, 171.4, 142.1, 141.7, 131.8, 131.1, 129.8, 127.0, 76.5, 76.0, 57.9, 57.6, 56.7, 43.5, 41.4, 40.2, 39.2, 37.2, 36.5, 36.4, 36.3, 34.0, 33.2, 33.1, 30.5, 29.2, 24.2, 22.0, 18.9, 14.3, 12.6. HR ESIMS *m/z* 708.2135 $[M - Na]^-$, $C_{31}H_{43}NNaO_{12}S_2^-$ requires 708.2124. HR ESIMS *m/z* 730.1927 $[M - Na]^-$, $C_{31}H_{42}NNa_2O_{12}S_2$ requires 730.1944.

Sodium 2β,3α-disulfate-5α-cholan-24-ol (7). Dry methanol (26 µL, 0.65 mmol) and $LiBH_4$ (325 µL, 2 M in THF, 0.65 mmol) were added to a solution of the methyl ester **2** (100 mg, 0.16 mmol) in dry THF (5 mL) at 0 °C under argon and the resulting mixture was stirred for 4 h at 0 °C. The mixture was quenched by addition of MeOH (2 mL) and then concentrated under *vacuo*. Purification by C18 silica gel eluting with H_2O–MeOH (7 : 3) gave the product **7** as a white solid (70 mg, 75%). An analytical sample was obtained by HPLC on a Nucleodur 100-5 C18 (5 µm; 4.6 mm i.d. × 250 mm, MeOH–H_2O 32 : 68, flow rate 1.5 mL min^{-1}, t_R = 3.2 min). $[\alpha]_{24}^{D}$ = +7.8 (*c* 0.24, CH_3OH); selected ^1H NMR (400 MHz CD_3OD): δ 4.69 (1H, br s), 4.74 (1H, br, s), 4.70 (1H, br s), 3.65 (1H, m), 3.50

(1H, m), 2.10 (1H, m), 2.00 (1H, m), 1.00 (3H, s), 0.95 (3H, d, J = 6.5 Hz), 0.69 (3H, s); ^{13}C NMR (100 MHz CD_3OD): δ 76.5, 76.2, 63.6, 57.9, 57.6, 56.6, 43.8, 41.5, 40.2, 39.1, 37.0, 36.4, 36.3, 33.2 (2C), 30.4, 30.3, 29.2, 29.1, 25.2, 22.0, 19.2, 14.3, 12.5; HR ESIMS m/z 559.2037 $[M - Na]^-$, $C_{24}H_{40}NaO_9S_2^-$ requires 559.2011.

5α-Cholest-2-ene (13). An oven-dried 250 mL flask was charged with 10% palladium on carbon (100 mg) and cholesterol (1.00 g, 2.6 mmol) and the flask was evacuated and flushed with argon. Absolute methanol (50 mL) and dry THF (50 mL) were added, and the flask was flushed with hydrogen. The reaction was stirred at room temperature under H_2 (1 atm) for 4 h. The mixture was filtered through celite and the recovered filtrate was concentrated. The residue was subjected to column chromatography on silica gel eluting with hexane–AcOEt (9 : 1) to give 950 mg of pure 5α-cholestan-3β-ol (90%). To a solution of this latter (950 mg, 2.4 mmol) in dry pyridine (50 mL), *p*-toluenesulfonyl chloride (1.3 g, 7.2 mmol) was added. The solution was stirred at room temperature for 24 h and then poured into cold water (30 mL) and extracted with CH_2Cl_2 (3 × 50 mL). The combined organic layer was washed with saturated $NaHCO_3$ solution (50 mL), and water (50 mL), and then dried over anhydrous $MgSO_4$ and evaporated in *vacuo* to give 1.2 g of residue, which was subjected to next step without any purification.

Lithium bromide (1.9 g, 22.0 mmol) and lithium carbonate (1.6 g, 22.0 mmol) were added to a solution of tosylate (1.2 g, 2.2 mmol) in dry DMF (150 mL), and the mixture was refluxed for 1.5 h. After cooling to room temperature, the mixture was slowly poured into 10% HCl solution (150 mL) and extracted with CH_2Cl_2 (3 × 150 mL). The combined organic layer was washed successively with water, saturated $NaHCO_3$ solution and water, and then dried over anhydrous $MgSO_4$ and evaporated to dryness to obtain pure **13** (773.3 mg, 87% over two steps). $[\alpha]_{24}^D$ = +52.5 (c 0.11, $CHCl_3$); selected ^{1}H NMR (400 MHz $CDCl_3$): δ 5.60 (2H, m), 0.91 (3H, d, J = 6.4 Hz), 0.87 (6H, d, J = 6.4 Hz), 0.75 (3H, s), 0.66 (3H, s). ^{13}C NMR (100 MHz $CDCl_3$): δ 126.0, 125.8, 56.4, 56.2, 54.0, 41.4, 40.0, 39.7, 39.5 (2C), 36.5, 36.1, 35.7, 35.6, 34.6, 31.8, 30.3, 28.7, 28.2, 28.0, 24.2, 22.8, 22.5, 20.9, 18.6, 12.0, 11.6; HR ESIMS m/z 393.3487 $[M + Na]^+$, $C_{27}H_{46}Na$ requires 393.3497.

2α,3α-Epoxy-5α-cholestane (14). To a solution of **13** (750 mg, 2.02 mmol) in $CHCl_3$ (50 mL) was added slowly *m*-chloroperbenzoic acid (488 mg, 2.8 mmol). The mixture was stirred for 4 h at room temperature, and then CH_2Cl_2 (50 mL) and 5% Na_2SO_3 solution (70 mL) were added. The CH_2Cl_2 phase was washed with water (70 mL), dried over anhydrous $MgSO_4$ and evaporated to dryness to give 560 mg of crude epoxide **14**, that was subjected to next step without any purification. Selected ^{1}H NMR (400 MHz $CDCl_3$): δ 3.16 (1H, br s), 3.11 (1H, br s), 0.88 (3H, d, J = 6.5 Hz), 0.85 (6H, d, J = 6.5 Hz), 0.73 (3H, s), 0.62 (3H, s); ^{13}C NMR (100 MHz $CDCl_3$): δ 56.2, 56.1, 53.6, 52.6, 51.3, 42.4, 40.0, 39.8, 39.5, 38.2, 36.2, 36.1, 35.7, 35.6, 33.6, 31.6, 29.0, 28.4, 28.2, 28.0, 24.2, 22.8, 22.5, 20.8, 18.6, 12.9, 11.9; HR ESIMS m/z 409.3458 ($[M + Na]^+$, $C_{27}H_{46}NaO$ requires 409.3446.

5α-Cholestan-2β,3α-diol (15). A solution of epoxide **14** (560 mg, 1.45 mmol) in THF (15 mL) was treated with 1N H_2SO_4 (3.6 mL, 3.6 mmol) solution and stirred for 24 h at room temperature. After neutralization with saturated $NaHCO_3$ solution, the mixture was evaporated to a fifth of the initial volume, diluted with water (50 mL), and extracted with ethyl acetate (3 × 50 mL). The combined organic extracts were washed with water, dried over anhydrous $MgSO_4$, filtered and evaporated to dryness. Purification on a silica gel column by eluting with hexane–AcOEt 7 : 3 afforded pure **15** (637 mg, 78% over two steps). $[\alpha]_{24}^D$ = +13.2 (c 0.2, CH_3OH); selected ^{1}H NMR (400 MHz CD_3OD): δ 3.90 (1H, br s), 3.87 (1H, br s), 0.90 (3H, d, J = 6.7 Hz), 0.87 (6H, d, J = 6.7 Hz), 0.80 (3H, s), 0.65 (3H, s); ^{13}C NMR (100 MHz CD_3OD): δ 72.1, 71.0, 56.7, 56.5, 55.4, 42.7, 40.5, 39.9, 39.5, 38.9, 36.2, 36.1, 35.8, 35.7, 35.3, 31.3, 31.0, 28.5, 28.2, 28.0, 24.1, 22.8, 22.5, 20.8, 18.6, 14.6, 12.0; HR ESIMS m/z 427.3572 ($[M + Na]^+$, $C_{27}H_{48}NaO_2$ requires 427.3552.

2β,3α-Cholestane disulfate (8). Triethylamine–sulfur trioxide complex (4.07 g, 22.5 mmol) was added to a solution of diol **15** (600 mg, 1.5 mmol) in DMF dry (70 mL) under an argon atmosphere, and the mixture was stirred at 95 °C for 48 h. Then, the reaction mixture was quenched with water (30 mL). The solution was poured over a C18 silica gel column to remove excess $Et_3N{\cdot}SO_3$. The product was eluted by MeOH and followed by evaporation of the solvent to yield a yellow solid [tris-(triethylammonium sulfate) salt]. To the solution of the solid in methanol (60 mL) was added Amberlite CG 120 sodium form (60 g). The mixture was stirred for 5 h at room temperature. The resin was removed by filtration, and the filtrate was concentrated to obtain compound **8** as a white solid (821 mg, 90%). An analytical sample was obtained by HPLC on a Nucleodur 100-5 C18 (5 μm; 4.6 mm i.d. × 250 mm, MeOH–H_2O 87 : 13, flow rate 1.5 mL min^{-1}, t_R = 2.6 min). $[\alpha]_{24}^D$ = +16 (c 0.2, CH_3OH); selected ^{1}H NMR (400 MHz CD_3OD): δ 4.75 (1H, m), 4.71 (1H, m), 0.97 (3H, s), 0.93 (3H, d, J = 6.4 Hz), 0.88 (6H, d, J = 6.4 Hz), 0.68 (3H, s); ^{13}C NMR (100 MHz CD_3OD): δ 76.5, 76.1, 57.8, 57.6, 56.6, 43.8, 41.4, 40.7, 40.2, 39.1, 37.3, 37.1, 36.4, 36.3, 31.8, 30.7, 30.5, 29.3, 29.1 (2C), 25.2, 23.2, 22.9, 22.0, 19.2, 14.3, 12.5; HR ESIMS m/z 585.2527 $[M - Na]^-$, $C_{27}H_{49}NaO_8S_2$ requires 585.2532.

Methyl 3α-hydroxy-5α-cholan-24-oate (17). To a solution of methyl 3β-hydroxy-5α-cholan-24-oate **16**[20] (173 mg, 0.44 mmol) in dry pyridine (30 mL), *p*-toluenesulfonyl chloride (420 mg, 2.2 mmol) was added. The solution was stirred at room temperature for 24 h and then poured into cold water (30 mL) and extracted with CH_2Cl_2 (3 × 50 mL). The combined organic layer was washed saturated $NaHCO_3$ solution (50 mL), and water (50 mL), and then dried over anhydrous $MgSO_4$ and evaporated in *vacuo* to give 200 mg of residue, that was subjected to next step without any purification.

A solution of methyl 3β-tosyl-5α-cholan-24-oate (200 mg, 0.36 mmol) and CH_3COOK (36 mg, 0.36 mmol) dissolved in water (1 mL) and DMF (7 mL) was refluxed for 5 h. The solution was cooled at room temperature and then ethyl acetate and water were added. The separated aqueous phase was extracted with ethyl acetate (3 × 30 mL). The organic phase was washed with water, dried (Na_2SO_4) and evaporated to dryness to give 190 mg of mixture, that was subjected to next step without any

purification. This residue was dissolved in 32 mL of mixture $CHCl_3$–MeOH (5 : 3) and *p*-toluensulfonic acid (*p*-TsOH) (619 mg, 3.6 mmol) was added. The mixture was quenched by addition of $NaHCO_3$ solution (30 mL) and then concentrated under *vacuo*. Ethyl acetate and water were added and the separated aqueous phase was extracted with ethyl acetate (3 × 50 mL). The combined organic phase was washed with water, dried (Na_2SO_4) and concentrated. Purification by silica gel eluting with hexane–AcOEt 99 : 1 gave the alcohol **17** as a white solid (130 mg, 75% over three steps). $[\alpha]_{24}^{D}$ = +7.2 (*c* 0.05, CH_3OH); selected ^{1}H NMR (400 MHz $CDCl_3$): δ 4.03 (1H, br s), 3.66 (3H, s), 2.35 (1H, m), 2.20 (1H, m), 0.90 (3H, d, *J* = 6.0 Hz), 0.77 (3H, s), 0.64 (3H, s); ^{13}C NMR (100 MHz $CDCl_3$): δ 175.3, 66.8, 56.8, 56.1, 54.6, 51.8, 42.8, 40.2, 40.0, 39.3, 36.1, 35.7, 35.6, 32.4, 32.2, 31.3, 31.2, 29.2, 28.8, 28.3, 24.4, 21.0, 18.5, 14.2, 12.3; HR ESIMS *m*/*z* 413.5867 $[M + Na]^+$, $C_{25}H_{42}NaO_3$ requires 413.5884.

5α-Cholan-3α,24-diyl-3,24-sodium disulfate (9). Dry methanol (70 μL, 1.8 mmol) and $LiBH_4$ (900 μL, 2 M in THF, 1.8 mmol) were added to a solution of the methyl ester **17** (100 mg, 0.25 mmol) in dry THF (10 mL) at 0 °C under argon and the resulting mixture was stirred for 4 h at 0 °C. The mixture was quenched by addition of MeOH (4 mL) and then concentrated under *vacuo*. Ethyl acetate and water were added and the separated aqueous phase was extracted with ethyl acetate (3 × 30 mL). The combined organic phase was washed with water, dried (Na_2SO_4) and concentrated to obtain 5α-cholan-3α,24-diol as a white solid (77 mg, 85%).

The triethylamine–sulfur trioxide complex (350 mg, 2 mmol) was added to a solution of diol (70 mg, 0.2 mmol) in DMF dry (2 mL) under an argon atmosphere, and the mixture was stirred at 95 °C for 24 h. Then, the reaction mixture was quenched with water (1.6 mL) and the solution was poured over a C18 silica gel column to remove excess $Et_3N{\cdot}SO_3$. The product was eluted by MeOH and followed by evaporation of the solvent to yield a yellow solid [tris-(triethylammonium sulfate) salt]. To the solution of the solid in methanol (4 mL) was added Amberlite CG 120 sodium form (2 g). The mixture was stirred for 5 h at room temperature. The resin was removed by filtration, and the filtrate was concentrated to obtain a residue that by purification on C18 [H_2O–MeOH (7 : 3)] gave the product **9** as a white solid (71.3 mg, 63%). An analytical sample was obtained by HPLC on a Nucleodur 100-5 C18 (5 μm; 4.6 mm i.d. × 250 mm, MeOH–H_2O 25 : 75, flow rate 1.5 mL min^{-1}, t_R = 2.4 min). $[\alpha]_{24}^{D}$ = + 0.42 (*c* 1.2, CH_3OH); selected ^{1}H NMR (400 MHz CD_3OD): δ 4.55 (1H, br s), 3.96 (2H, m), 0.90 (3H, d, *J* = 6.5 Hz), 0.80 (3H, s), 0.65 (3H, s); ^{13}C NMR (100 MHz CD_3OD): δ 76.5, 69.7, 57.9, 57.6, 55.1, 43.8, 41.6, 41.4, 40.8, 36.9, 36.8, 34.7, 33.8, 33.2, 33.1, 29.6, 29.2, 27.9, 27.2, 25.2, 21.9, 19.0, 14.4, 12.5. HR ESIMS *m*/*z* 543.2078 $[M - Na]^-$, $C_{24}H_{40}NaO_8S_2$ requires 543.2062.

5α-Cholan-3β,24-diyl-3,24-sodium disulfate (10). Dry methanol (10 μL, 0.20 mmol) and $LiBH_4$ (100 μL, 2 M in THF, 0.20 mmol) were added to a solution of the methyl ester **16** (20 mg, 0.05 mmol) in dry THF (2 mL) at 0 °C under argon and the resulting mixture was stirred for 4 h at 0 °C. The mixture was quenched by addition of MeOH (2 mL) and then allowed to warm to room temperature and concentrated under *vacuo*. Ethyl acetate and water were added and the separated aqueous phase was extracted with ethyl acetate (3 × 30 mL). The combined organic phases were washed with water, dried (Na_2SO_4) and concentrated to obtain 5β-cholan-3α,24-diol as a white solid (13 mg, 72%).

The triethylamine–sulfur trioxide complex (63 mg, 0.35 mmol) was added to a solution of diol (13 mg, 0.035 mmol) in DMF dry (2 mL) under an argon atmosphere, and the mixture was stirred at 95 °C for 3 h. The resulting solution was concentrated under reduced pressure. To the solution of the solid in methanol (3 mL) was added Amberlite CG 120 sodium form (1 g). The mixture was stirred for 5 h at room temperature. The resin was removed by filtration, and the filtrate was concentrated and then diluted with water and loaded onto a C18 silica gel column, which was washed with water (50 mL). Elution with 30% aqueous methanol gave the compound **10** as a white solid (15 mg, 78%). An analytical sample was obtained by HPLC on a Nucleodur 100-5 C18 (5 μm; 4.6 mm i.d. × 250 mm, MeOH–H_2O 25 : 75, flow rate 1.5 mL min^{-1}, t_R = 2.4 min). $[\alpha]_{24}^{D}$ = +6.4 (*c* 1.0, CH_3OH); selected ^{1}H NMR (400 MHz CD_3OD): δ 4.59 (1H, m), 3.95 (1H, br s), 0.95 (3H, d, *J* = 6.0 Hz), 0.82 (3H, s), 0.78 (3H, s); ^{13}C NMR (100 MHz CD_3OD): δ 79.9, 64.3, 57.9, 57.6, 55.4, 43.8, 41.4 (2C), 38.2, 36.8, 36.7, 36.3, 33.3, 33.1, 32.2, 30.7, 29.2, 28.7, 27.1, 25.2, 22.3, 19.0, 14.4, 12.5. HR ESIMS *m*/*z* 543.2075 $[M - Na]^-$, $C_{24}H_{40}NaO_8S_2$ requires 543.2062.

Transactivation assay. HepG2 cells were transfected using Fugene HD transfection reagent (Roche). The plasmids used for luciferase assay were pSG5-PXR, pSG5-RXR, pCMV-βgalactosidase and the reporter vector p(CYP3A4)-TK-Luc. 48 h post-transfection cells were stimulated 18 h and than lysed in 100 μL diluted reporter lysis buffer (Promega). 20 μL of cellular lysates were read using the Luciferase Substrate (Promega). Luminescence was measured using the Glomax 10/10 luminometer (Promega). Luciferase activities were normalized for transfection efficiencies by dividing the relative light units by β-galactosidase activity expressed from cotransfected pCMV-βgal.

Cell culture. HepG2 cells were maintained at 37 °C in E-MEM containing 10% fetal bovine serum (FBS), 1% L-glutamine and 1% penicillin/streptomycin. HepG2 cells were stimulated 18 h with 10 μM rifaximin **1** and compounds **2–10** and relative mRNA levels of CYP3A4 were analyzed by Real-Time PCR.

HSC-T6, a rat immortalised HSC line, was cultured at 37 °C in an atmosphere of 5% CO_2 in Dulbecco's modified minimal essential medium containing 10% FBS, 2 mmol L^{-1} L-glutamine, 5000 IU mL^{-1} penicillin and 5000 g mL^{-1} streptomycin. After 72 h serum starvation, cells were stimulated with 10 μM solomonsterol A (**1**) or compound **8** alone or in combination of 10 U mL^{-1} thrombin. Total RNA was extracted to assess the relative mRNA levels of alpha smooth muscle actin (αSMA) by quantitative Real-Time PCR.

THP-1 cells were maintained at 37 °C in RPM-I containing 10% fetal bovine serum (FBS), 1% L-glutamine and 1% penicillin/streptomycin. Cells were serum starved for 24 h and pre-treated with 10 μM of compound **8** for 3 h before the addition of

1 μg mL^{-1} LPS. After 18 h-stimulation total RNA was extracted to assess the relative mRNA levels of IL1β, TNFα and MCP-1 by Real-Time PCR.

Real-time PCR. Total RNA was extracted using the TRIzol reagent (Invitrogen), purified of the genomic DNA by DNAase I treatment (Invitrogen) and random reverse-transcribed with Superscript II (Invitrogen). Fifty ng template was amplified using the following reagents: 0.2 μM of each primer and 12.5 μL of 2×SYBR Green qPCR master mix (Invitrogen). All reactions were performed in triplicate and the thermal cycling conditions were: 2 min at 95 °C, followed by 40 cycles of 95 °C for 20 s, 55 °C for 20 s and 72 °C for 30 s in iCycler iQ instrument (Biorad). The relative mRNA expression was calculated and expressed as $2^{-(\Delta\Delta Ct)}$. Primers used for qRT-PCR were: hGAPDH: GAAGGTGAAGGTCGGAGT and CATGGGTGGAATCATATTGGAA; hCYP3A4: CAAGACCCCTTTGTGGAAAA and CGAGGCGACTTTCTTTCATC; hIL1β: GGACAAGCTGAGGAAGATGC and TCGTTATCCCATGTGTCGAA; hTNFα: AACCTCCTCTCTGCCATCAA and GGAAGACCCCTCCCAGATAG; hMCP-1: CCCCAGTCACCTGCTGTTAT and TCCTGAACCCACTTCTGCTT; rGAPDH: ATGACTCTACCCACGGCAAG and TACTCAGCACCAGCATCACC; rαSMA: GCTCCATCCTGGCTTCTCTA and TAGAAGCATTTGCGGTGGAC.

Computational details. Prior to docking calculations, we built and processed the chemical structures of the compounds with Macromodel 8.5 (Schrödinger, LLC, New York, 2003). Molecular mechanics/dynamics calculations were performed on a 4× AMD Opteron SixCore 2.4 GHz using Macromodel 8.5 and the OPLS force field. The Monte Carlo multiple minimum (MCMM) method (5000 steps) was used first in order to allow a full exploration of the conformational space. Molecular Dynamics simulations were performed at 600 K and with a simulation time of 10 ns. A constant dielectric term, mimicking the presence of the solvent, was used in the calculations to reduce artifacts. Finally, we applied an optimization (Conjugate Gradient, 0.05 Å convergence threshold) of the structures for the identification of a possible three-dimensional starting models for the subsequent steps of docking calculations by Autodock 4.2 software. A grid box size of 90 × 108 × 96 with spacing of 0.375 Å between the grid points and centered at 14.282 (x), 74.983 (y), and 0.974 (z) was used for the PXR receptor. We performed 10 calculations consisting of 256 runs, obtaining 2560 structures (256 × 10), using the Lamarckian genetic algorithm for dockings. An initial population of 450 randomly placed individuals, a maximum number of 5.0×10^6 energy evaluations, and a maximum number of 6.0×10^6 generations were taken into account. A mutation rate of 0.02 and a crossover rate of 0.8 were used. We clustered together results differing by less than 3.0 Å in positional root-mean-square deviation (rmsd). For all the investigated compounds, all open-chain bonds were treated as active torsional bonds. Docking results were analyzed with Autodock Tools 1.4.5. Illustrations of the 3D models were generated using the Python software.[40]

Acknowledgements

This work was supported by grants from MAREX-Exploring Marine Resources for Bioactive Compounds: From Discovery to Sustainable Production and Industrial Applications (Call FP7-KBBE-2009-3, Project nr. 245137) and from MIUR (PRIN 2009) "Sostanze ad attività antitumorale: isolamento da fonti marine, sintesi di analoghi e ulteriore sviluppo della chemoteca LIBIOMOL" and "Design, conformational and configurational analysis of novel molecular platforms" and from the University of Salerno (FARB ex 60%). NMR spectra were provided by the CSIAS, Centro Interdipartimentale di Analisi Strumentale, Faculty of Pharmacy, University of Naples.

References

1 K. L. Rock, E. Latz, F. Ontiveros and H. Kono, *Annu. Rev. Immunol.*, 2010, **28**, 321.
2 X. Ma, Y. M. Shah, G. L. Guo, T. Wang, K. W. Krausz, J. R. Idle and F. J. Gonzalez, *J. Pharmacol. Exp. Ther.*, 2007, **322**, 391.
3 S. Fiorucci, S. Cipriani, F. Baldelli and A. Mencarelli, *Prog. Lipid Res.*, 2010, **49**, 171.
4 A. Mencarelli, M. Migliorati, M. Barbanti, S. Cipriani, G. Palladino, E. Distrutti, B. Renga and S. Fiorucci, *Biochem. Pharmacol.*, 2010, **80**, 1700.
5 W. Xie and Y. Tian, *Cell Metab.*, 2006, **4**, 177.
6 C. Zhou, M. M. Tabb, E. L. Nelson, F. Grün, S. Verma, A. Sadatrafiei, M. Lin, S. Mallick, B. M. Forman, K. E. Thummel and B. Blumberg, *J. Clin. Invest.*, 2006, **116**, 2280.
7 T. Langmann, C. Moehle, R. Mauerer, M. Scharl, G. Liebisch, A. Zahn, W. Stremmel and G. Schmitz, *Gastroenterology*, 2004, **127**, 26.
8 A. S. Day and R. B. Gearry, *Dig. Dis. Sci.*, 2010, **55**, 877.
9 J. Cheng, Y. M. Shah, X. Ma, X. Pang, T. Tanaka, T. Kodama, K. W. Krausz and F. J. Gonzalez, *J. Pharmacol. Exp. Ther.*, 2010, **335**, 32.
10 Z. D. Jiang, S. Ke and H. L. DuPont, *Int. J. Antimicrob. Agents*, 2010, **35**, 278.
11 V. Sepe, G. Bifulco, B. Renga, C. D'Amore, S. Fiorucci and A. Zampella, *J. Med. Chem.*, 2011, **54**, 1314.
12 S. De Marino, R. Ummarino, M. V. D'Auria, M. G. Chini, G. Bifulco, B. Renga, C. D'Amore, S. Fiorucci, C. Debitus and A. Zampella, *J. Med. Chem.*, 2011, **54**, 3065.
13 S. De Marino, V. Sepe, M. V. D'Auria, G. Bifulco, B. Renga, S. Petek, S. Fiorucci and A. Zampella, *Org. Biomol. Chem.*, 2011, **9**, 4856.
14 V. Sepe, R. Ummarino, M. V. D'Auria, M. G. Chini, G. Bifulco, B. Renga, C. D'Amore, C. Debitus, S. Fiorucci and A. Zampella, *J. Med. Chem.*, 2012, **55**, 84.
15 B. Renga, A. Mencarelli, C. D'Amore, S. Cipriani, M. V. D'Auria, V. Sepe, M. G. Chini, M. C. Monti, G. Bifulco, A. Zampella and S. Fiorucci, *PLoS One*, 2012, **7**, e30443.
16 M. G. Chini, C. R. Jones, A. Zampella, M. V. D'Auria, B. Renga, S. Fiorucci, C. P. Butts and G. Bifulco, *J. Org. Chem.*, 2012, **77**, 1489.
17 S. De Marino, R. Ummarino, M. V. D'Auria, M. G. Chini, G. Bifulco, C. D'Amore, B. Renga, A. Mencarelli, S. Petek, S. Fiorucci and A. Zampella, *Steroids*, 2012, **77**, 484.
18 C. Festa, S. De Marino, M. V. D'Auria, G. Bifulco, B. Renga, S. Fiorucci, S. Petek and A. Zampella, *J. Med. Chem.*, 2011, **54**, 401.
19 Y. M. Shah, X. Ma, K. Morimura, I. Kim and F. J. Gonzalez, *Am. J. Physiol.*, 2007, **292**, G1114.
20 V. Sepe, R. Ummarino, M. V. D'Auria, A. Mencarelli, C. D'Amore, B. Renga, A. Zampella and S. Fiorucci, *J. Med. Chem.*, 2011, **54**, 4590.
21 C. Rousseaux, B. Lefebvre, L. Dubuquoy, P. Lefebvre, O. Romano, J. Auwerx, D. Metzger, W. Wahli, B. Desvergne, G. C. Naccari, P. Chavatte, A. Farce, P. Bulois, A. Cortot, J. F. Colombel and P. Desreumaux, *J. Exp. Med.*, 2005, **201**, 1205.
22 M. Kunishima, C. Kawachi, K. Hioki, K. Terao and S. Tani, *Tetrahedron*, 2001, **57**, 1551.
23 R. E. Watkins, G. B. Wisely, L. B. Moore, J. L. Collins, M. H. Lambert, S. P. Williams, T. M. Willson, S. A. Kliewer and M. R. Redinbo, *Science*, 2001, **292**, 2329.

24 S. Ekins, S. Kortagere, M. Iyer, E. J. Reschly, M. A. Lill, M. R. Redinbo and M. D. Krasowski, *PLoS Comput. Biol.*, 2009, **5**, e1000594.
25 G. A. G. Santos, A. P. Murray, C. A. Pujol, E. B. Damonte and M. S. Maier, *Steroids*, 2003, **68**, 125.
26 R. Cong, Y. Zhang and W. Tian, *Tetrahedron Lett.*, 2010, **51**, 3890.
27 K. Wang, I. Damjanov and Y. J. Wan, *Lab. Invest.*, 2010, **90**, 257.
28 C. J. Marek, S. J. Tucker, D. K. Konstantinou, L. J. Elrick, D. Haefner, C. Sigalas, G. I. Murray, B. Goodwin and M. C. Wright, *Biochem. J.*, 2005, **387**, 601.
29 B. Renga, A. Mencarelli, M. Migliorati, S. Cipriani, C. D'Amore, E. Distrutti and S. Fiorucci, *Inflammation Res.*, 2011, **60**, 577.
30 S. Fiorucci, E. Antonelli, G. Rizzo, B. Renga, A. Mencarelli, L. Riccardi, S. Orlandi, R. Pellicciari and A. Morelli, *Gastroenterology*, 2004, **127**, 1497.
31 S. Fiorucci, E. Antonelli, E. Distrutti, B. Severino, R. Fiorentina, M. Baldoni, G. Caliendo, V. Santagada, A. Morelli and G. Cirino, *Hepatology*, 2004, **39**, 365.
32 G. M. Morris, R. Huey, W. Lindstrom, M. F. Sanner, R. K. Belew, D. S. Goodsell and A. J. Olson, *J. Comput. Chem.*, 2009, **30**, 2785.
33 R. E. Watkins, J. M. Maglich, L. B. Moore, G. B. Wisely, S. M. Noble, P. R. Davis-Searles, M. H. Lambert, S. A. Kliewer and M. R. Redinbo, *Biochemistry*, 2003, **42**, 1430.
34 L. Xiao, E. Nickbarg, W. Wang, A. Thomas, M. Ziebell, W. W. Prosise, C. A. Lesburg, S. S. Taremi, V. L. Gerlach, H. V. Le and K. C. Cheng, *Biochem. Pharmacol.*, 2011, **81**, 669.
35 A. Mencarelli, B. Renga, G. Palladino, D. Claudio, P. Ricci, E. Distrutti, M. Barbanti, F. Baldelli and S. Fiorucci, *Eur. J. Pharmacol.*, 2011, **668**, 317.
36 M. Trauner and E. Halilbasic, *Gastroenterology*, 2011, **140**, 1120.
37 S. Kakizaki, D. Takizawa, H. Tojima, N. Horiguchi, Y. Yamazaki and M. Mori, *Front. Biosci.*, 2011, **17**, 2988.
38 E. L. Haughton, S. J. Tucker, C. J. Marek, E. Durward, V. Leel, Z. Bascal, T. Onaghan, M. Koruth, E. Collie-Duguid, D. A. Mann, J. E. Trim and M. C. Wright, *Gastroenterology*, 2006, **131**, 194.
39 G. Rizzo, M. Disante, A. Mencarelli, B. Renga, A. Gioiello, R. Pellicciari and S. Fiorucci, *Mol. Pharmacol.*, 2006, **70**, 1164.
40 M. F. Sanner, *J. Mol. Graphics Modell.*, 1999, **17**, 57.

